Journal of Nuclear and Radiochemical Sciences, Vol. 25, pp. 1-5, 2026

Articles

^{99}Ru Synchrotron-Radiation-Based Mössbauer Spectroscopy of Na_2RuO_3

Mio Yoshida[1], Ryo Masuda[2], Nobumoto Nagasawa[3], Satoshi Tsutsui[3,4]
Jin Nakamura[1], Yoshio Kobayashi *[1,5,6]

[1] *Department of Fundamental Science and Engineering, University of Electro-Communications, Chofu, Tokyo 182-8585, Japan*
[2] *Graduate School of Science and Technology, Hirosaki University, Hirosaki, Aomori 036-8561, Japan*
[3] *Japan Synchrotron Radiation Research Institute (JASRI), SPring-8, Sayo, Hyogo 679-5198, Japan*
[4] *Institute of Quantum Beam Science, Graduate School of Science Engineering, Ibaraki University, Hitachi, Ibaraki 316-8511, Japan*
[5] *Division of Arts and Sciences, International Christian University, Mitaka, Tokyo 181-8585, Japan*
[6] *RIKEN Nishina Center for Accelerator-Based Science, Wako, Saitama 351-0198, Japan*

Received November 10, 2025; Accepted December 2, 2025; Published online August 26, 2026

Improved ^{99}Ru synchrotron-radiation-based (SR) Mössbauer spectroscopy technique was applied to Ru metal and Na_2RuO_3, a promising cathode material for sodium-ion rechargeable batteries. The ^{99}Ru Mössbauer spectrum of Na_2RuO_3 exhibited an isomer shift characteristic of Ru^{4+} ions. In electrochemically desodiated $Na_{2-x}RuO_3$, the Na-deficient Na_1RuO_3 was partially formed via one-electron oxidation, and its oxidation state was identified as Ru^{5+}. It was found that the pronounced nuclear quadrupole splitting observed in $Na_{2-x}RuO_3$ arises from the distorted RuO_6 octahedra, as confirmed in X-ray diffraction powder pattern, caused by Na deficiency. These findings demonstrate that ^{99}Ru SR-based Mössbauer spectroscopy is a highly sensitive and effective tool for probing electronic and structural changes induced by redox processes in ruthenium compounds.

Keywords: *^{99}Ru Mössbauer spectroscopy; Synchrotron-radiation-based Mössbauer spectroscopy; Na_2RuO_3; Na deficiency; Ru^{4+}; Ru^{5+}*

1. Introduction

Mössbauer spectroscopy, as an element-specific analytical technique for chemical and physical properties, has traditionally been conducted with radioactive sources before Ruby's proposal.[1] Those work using radioactive sources have been prepared commercially or produced through nuclear reactions at nuclear reactors or accelerators. However, recent development of synchrotron radiation techniques enables us to measure energy-domain Mössbauer spectra like those obtained by conventional Mössbauer spectroscopy using high-intense X-ray source delivered by synchrotron radiation facilities instead of radioactive sources.[2] This method, called synchrotron-radiation-based (SR-based) Mössbauer spectroscopy, is applicable even in the absence of radioactive sources as their parent nuclei. This development has opened up new avenues for applying Mössbauer spectroscopy to rare yet valuable elements that have previously received little attention. With this development, SR-based Mössbauer spectroscopy has been demonstrated for ^{149}Sm (E_γ = 22.5 keV)[3], ^{61}Ni (E_γ = 67.4 keV)[4], ^{193}Ir (E_γ = 73.0 keV)[5], ^{174}Yb (E_γ = 76.5 keV)[6] and ^{158}Gd (E_γ = 79.5 keV)[7], thereby increasing the number of accessible Mössbauer transitions and broadening the fields of related scientific and industrial applications.

Ruthenium, one of the elements extensively employed in functional materials of catalysts, battery materials, electronic devices, and so on, exhibits a wide variety of chemically stable oxidation states ranging from –2 to +8. The information provided by ^{99}Ru Mössbauer spectra should be highly valuable for materials science research. The Mössbauer effect of ^{99}Ru was first reported by Kistner in 1963[8] and the detailed investigation was also published in 1966.[9] Despite the usefulness of ^{99}Ru Mössbauer spectroscopy, the limited number of applications reported since his pioneering works can be attributed to the following reasons. First, the Mössbauer source nuclide ^{99}Rh has a relatively short half-life of 16 days and the production of ^{99}Rh requires a proton accelerator for the ^{99}Ru(p,n)^{99}Rh nuclear reaction.[9,10] Additionally, since the resonant energy of the ^{99}Ru Mössbauer transition is as high as 89.6 keV, both the source and the absorber must be cooled and maintained near liquid helium temperatures in order to observe the resonance absorption line. These are the main reasons why ^{99}Ru Mössbauer spectroscopy has not been as widely utilized like ^{57}Fe and ^{119}Sn Mössbauer spectroscopy. However, owing to the relatively long lifetime of the first excited state of 20.5 ns, a natural linewidth (Γ_0 = 0.149 mm s^{-1}) comparable to that of ^{57}Fe or ^{119}Sn can be achieved, making ^{99}Ru Mössbauer spectroscopy widely applicable to materials science.[10] Such a relatively narrow linewidth makes the technique highly sensitive to precise observation of hyperfine interactions. In particular, because Ru atoms can occupy valence states ranging from Ru^{2-} to Ru^{8+}, the resulting spread of observable isomer shifts exceeds the natural linewidth of ^{99}Ru, allowing precise discussion of multiple Ru valence states.

This study aims a development and an application of ^{99}Ru SR-based Mössbauer spectroscopy to advanced material science. First, based on the previous study by Masuda et al.,[7] the ^{99}Ru SR-based Mössbauer spectrometry was improved and optimized by introducing a channel-cut filter and lowering the temperature of a scatterer to obtain a high-quality spectrum. We have conducted ^{99}Ru SR-based Mössbauer spectroscopy of Ru metal, the standard of the isomer shifts in ^{99}Ru Mössbauer spectroscopy. Then, the improved ^{99}Ru SR-based Mössbauer spectroscopy has subsequently been applied to Na_2RuO_3 as a candidate cathode material for sodium-ion rechargeable batteries (SIB).[11-20] The purpose of this study was to elucidate the oxidation states and coordination

*Corresponding author. E-mail: yoshio.kobayashi@uec.ac.jp

Published on Web 08/26/2026

environments of the Ru sites in Na_2RuO_3, which were closely related to the charge–discharge characteristics of the cathode material. The change in the oxidation state of Ru after electrochemical charging was clearly reflected in the isomer shift in the ^{99}Ru Mössbauer spectrum. The coordination environment around Ru was clarified by combining the quadrupole splitting observed in the ^{99}Ru Mössbauer spectrum with X-ray diffraction analysis.

2. Experimental Procedure

Sample Preparation

The ^{99}Ru metal powder with an enrichment of 97.69 % was used either as a transmitter of ^{99}Ru SR-based Mössbauer measurement or as a starting material for the synthesis of Na_2RuO_3. ^{99}Ru enriched RuO_2 as a starting material for Na_2RuO_3 was obtained by heating ^{99}Ru metal powder in air at 850 °C for 14 h. Then, Na_2RuO_3 was synthesized by a conventional solid-state reaction, in which RuO_2 and $NaHCO_3$ were stoichiometrically mixed, pelletized, and sintered at 850 °C for 48 h under an Ar atmosphere.[12,14]

A portion of Na_2RuO_3 was electrochemically desodiated by charging to obtain Na-deficient $Na_{2-x}RuO_3$. Na_2RuO_3 was used as the cathode and hard carbon as the anode in a flat cell, respectively, and a constant voltage of 4 V was applied for 30 min for charging.[14,21] The X-ray powder diffraction patterns (XRD) of Na_2RuO_3 and $Na_{2-x}RuO_3$ were measured using Rigaku SmartLab diffractometer equipped with Cu *K*α radiation

^{99}Ru SR-based Mössbauer spectrometry

^{99}Ru SR-based Mössbauer spectroscopy was performed at BL35XU of SPring-8, Japan, using an experimental setup nearly identical to that used for ^{61}Ni and ^{193}Ir SR-based Mössbauer spectroscopy, as shown in Fig. 1.[4,5] X-ray optics consisted of a Si(3 3 3) double-crystal beamline monochromator and a Si(8 8 0) channel-cut crystal. The Si(8 8 0) crystal simultaneously eliminates the contribution of X-rays monochromatized by Si(1 1 1) and also reduced the incident bandwidth of X-rays' energy to 0.38 eV in order to prevent the overloading of the detection system and improve the signal-to-noise ratio.

The avalanche photodiode detector (APD) with sufficient time resolution was used to distinguish ^{99}Ru nuclear-resonance signals from electronic scattering ones from the sample. Since the internal conversion coefficient α of ^{99}Ru was reported to be 1.50 in the transition of 89.6 keV resonance,[10,22] APD detectors were located just over the scatterer for effectively accumulating the signals of the conversion fluorescence X-rays, and the conversion electrons as well as the resonant X-rays after de-exciting ^{99}Ru nuclei.[6,7,23,24] The 11 bunch × 29 train on the operation mode of SPring-8, whose pulse interval between each train and the current per bunch are 145.5 ns and 0.31 mA,[25] was also chosen for distinguishing the ^{99}Ru nuclear-resonance signals from the electronic scattering one, because the half-life of the first excited state in ^{99}Ru is 20.5 ns.

Mössbauer measurements using high-energy transitions, such as the 89.6 keV ^{99}Ru resonance, generally require low temperatures for both source and sample because of the large recoil energies. In the present work, two closed-cycle helium cryostats were used to cool the scatterer instead of a radioactive source in conventional measurements and the sample independently. Because the observed spectral intensity is proportional to the product of the recoil-free fractions of the scatterer and the sample, this cooling setup increases the detected spectral intensity. Placing the scatterer and sample sufficiently far apart in this setup also reduces geometrical Doppler broadening. The scatterer was a pellet of ^{99}Ru enriched metal powder with an enrichment of 97.69 %, mixed with boron nitride to improve its thermal conductivity. The scatterer was mounted on a copper holder in the cryostat. The scatterer and sample temperatures were maintained at 11 K and 7 K, respectively, allowing clear observation of hyperfine interactions.

The velocity transducer was operated using triangular wave provided by a function generator. Velocity calibration of the system was done by the laser interferometer. Zero velocity was referred to the isomer shift of Ru metal.

3. Results and Discussion

^{99}Ru SR-based Mössbauer spectroscopy of Ru metal

The ^{99}Ru SR-based Mössbauer spectrum of ^{99}Ru enriched metal powder was measured at 7 K, as shown in Fig. 2. The total acquisition time was 3.3 h. The spectrum showed a single-line absorption peak without any sign of electric quadrupole or magnetic hyperfine interactions below 7 K. Although the spectral profile can be described by the equation given in Ref. 26, this shape is caused by the time window effect known in delayed coincidence Mössbauer spectroscopy.[27, 28] In the present case of ^{99}Ru SR-based Mössbauer spectroscopy using the 11 bunch x 29 train operation, the resonant line profile can be approximated by a Lorentzian function because the longer X-ray pulse interval eliminates the structure of the resonance line tail, as shown in Ref. 3. Therefore, the obtained spectra were successfully analyzed using the MossWinn program.[29]

The resonance absorption peak was observed to be 8.7%, which was approximately five times higher than 1.6 % obtained using a radioactive ^{99}Rh source.[30] In the SR-based Mössbauer spectroscopy, non-resonant radiations, which are present when using a radioactive source, are effectively eliminated by means of the beamline monochromator and channel-cut crystals. This suppression of background radiation enhances both the energy and spatial selectivity, resulting in an increased resonant absorption efficiency. Installation of appropriate channel-cut crystals in the beamline optics and improvement of thermal conductivity in

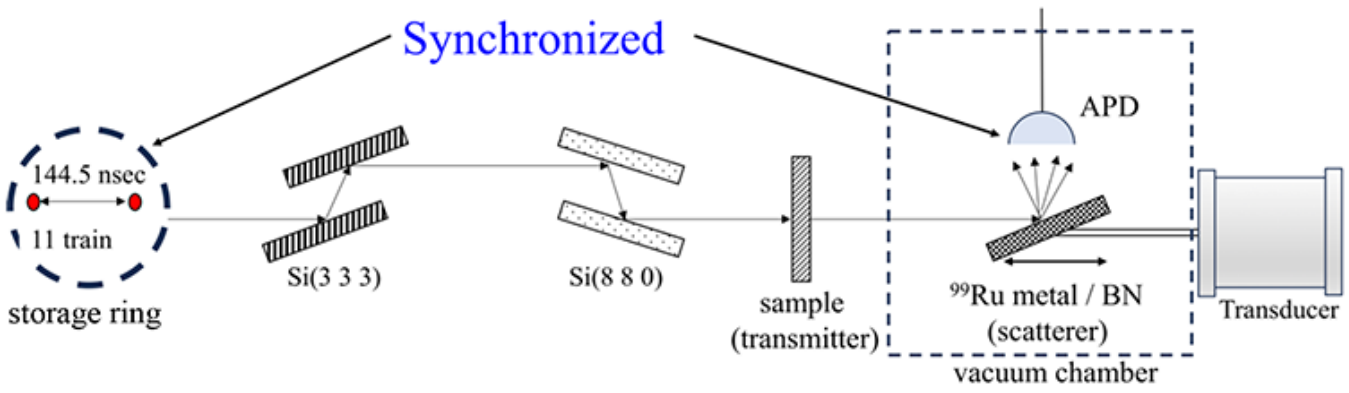

Figure 1. Schematic drawing of the setup for ^{99}Ru SR-based Mössbauer spectroscopy at BL35XU of SPring-8. The temperatures of sample (transmitter) and ^{99}Ru metal (scatterer) were kept at 7 K and 11 K, respectively.

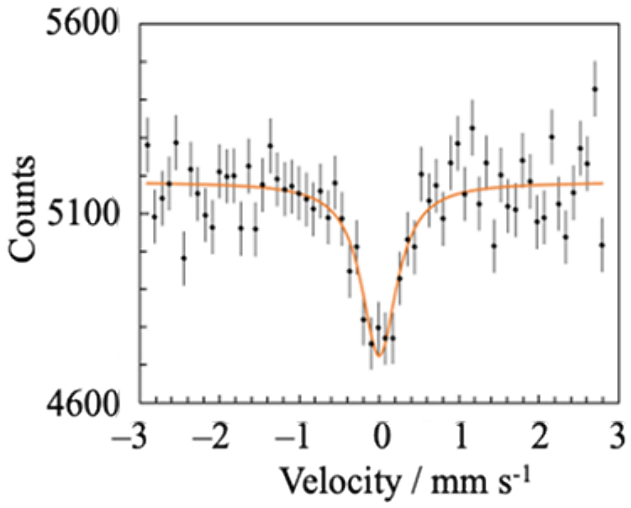

Figure 2. ^{99}Ru SR-based Mössbauer spectrum of ^{99}Ru enriched metal measured at 7 K.

the scatter allow us to observe the spectral intensities in the present work more than those in the previous work.[4] However, the linewidth (FWHM) was 0.36±0.11 mm s^{-1}, which was more than 40% broader than the 0.25±0.01 mm s^{-1} observed in the radioactive source experiment.[30] Under identical conditions of the recoil-free fraction, f_a, the absorber thickness, t_a, and measurement temperature, the effective thickness of the Mössbauer resonant absorption, T, is proportional to the areal density of the Mössbauer isotope in the absorber, n_a. For a thin effective thickness, the observed spectral linewidth, Γ_{obs}, approaches the natural linewidth, Γ_0. According to calculations based on the description by Greenwood et al.,[31] the observed linewidth Γ_{obs} in this study using an enriched Ru metal was estimated to be approximately 50 % broader than that obtained with a sample of natural isotopic abundance of 12.8 %. This indicates that the observed linewidth broadening in our ^{99}Ru SR-based Mössbauer spectra originated from the use of the enriched stable isotope. Success of observing the ^{99}Ru SR-based Mössbauer spectrum of Ru metal makes ^{99}Ru Mössbauer spectra feasible in various Ru compounds.

Characterization by XRD of Na_2RuO_3 and Na-deficient $Na_{2-x}RuO_3$ after charging

The X-ray powder diffraction pattern (XRD) of Na_2RuO_3 is shown in Fig. 3 (a). The diffraction pattern was identified as a layered compound with a rhombohedral structure (space group *R3m*), as reported by de Boisse et al.[14,16] No reflections corresponding to unreacted RuO_2, other ruthenium compounds, oxide or by-products were detected. The crystal structure of Na_2RuO_3 belongs to the O3-type layered family, in which slightly distorted RuO_6 octahedral layers alternate with NaO_6 octahedral layers along the *c*-axis. In O3-Na_2RuO_3, the NaO_6 octahedron in Na layers shares edges with two NaO_6 and four RuO_6 octahedra in the adjacent $[Ru_{2/3}Na_{1/3}]O_2$ layers.[14,16] From the 2θ position of the (0 0 3) reflection, the interplanar spacing was calculated to be 5.405 Å. The corresponding *c*-axis length of the O3-Na_2RuO_3 unit cell was estimated as 16.21 Å, which agrees with previously reported values within a relative error of 3 %.[14,32]

Upon charging, our XRD pattern of Na-deficient $Na_{2-x}RuO_3$ showed the characteristic (0 0 3) reflection for the layered structure shifted to a higher 2θ angle and new peaks appeared, as shown in Fig. 3 (b). During electrochemical desodiation induced by charging, partial deintercalation of Na^+ ions occurred from the NaO_6 octahedron layer, leading to the formation of Na-deficient Na_1RuO_3, within the $[Ru_{2/3}Na_{1/3}]O_2$ layers.[14,16] However, since the layered honeycomb framework was preserved, the shortening of the interlayer spacing resulted in the (0 0 3) reflection shifting to a higher angle. As the result, the interlayer distance decreased from 5.405 Å to 5.197 Å. The reflection at 2θ = 26° was a residue of ethylene carbonate used in the electrolysis.

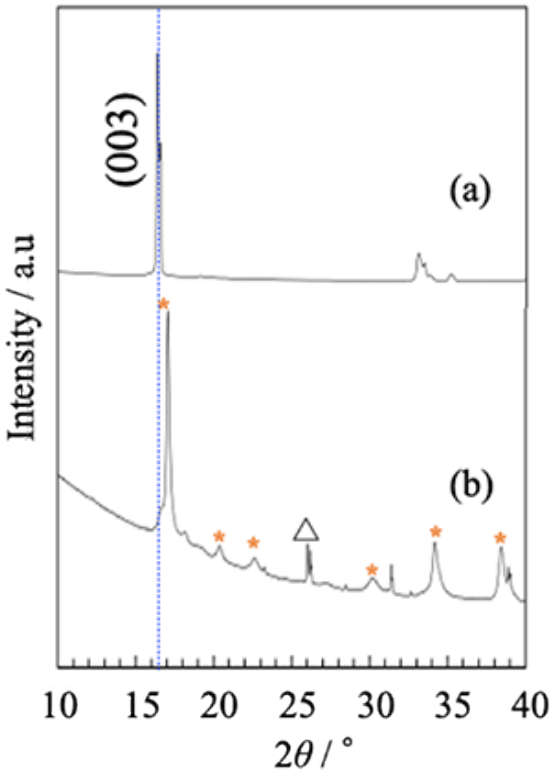

Figure 3. X-ray powder diffraction patterns of (a) Na_2RuO_3 and (b) Na-deficient $Na_{2-x}RuO_3$ obtained after charging. The asterisks (∗) and triangles (△) indicate reflections arising from Na-deficient Na_1RuO_3 and ethylene carbonate, respectively.

^{99}Ru SR-based Mössbauer spectroscopy of Na_2RuO_3 and Na-deficient $Na_{2-x}RuO_3$ after charging

The ^{99}Ru SR-based Mössbauer spectra of Na_2RuO_3 and Na-deficient $Na_{2-x}RuO_3$ after electrochemical charging were measured under the same experimental conditions as for Ru metal. The Mössbauer spectrum of Na_2RuO_3 at 7 K is shown in Fig. 4 (a). The spectrum could be satisfactorily fitted with an apparent doublet with a small asymmetry, characteristic of an electric quadrupole interaction without magnetic ordering. The derived isomer shift δ (relative to ruthenium metal) and the quadrupole splitting ΔE_Q (defined by $e^2qQ_e/2$) were –0.29±0.04 mm s^{-1} and –0.43±0.05 mm s^{-1}, respectively. This analysis was consistent with the results of Veiga et al. that Na_2RuO_3 exhibits temperature-independent Pauli paramagnetism down to 1.5 K, based on magnetic susceptibility and neutron scattering measurements.[32] The value of the isomer shift was in the typical tetravalent state, corresponding to a low-spin $4d^4$ configuration,[33,34] and agreed with our previous work using ^{99}Rh source.[14]

Although the spectrum resembles a doublet, it actually comprises six resonance lines corresponding to the E2/M1 transition from I_e = 3/2 to I_g = 5/2 of ^{99}Ru nuclei when the electric field gradient (EFG) tensors are small.[9,10,35] However, when the electric field gradient tensor becomes sufficiently large, the contribution from the ground-state nuclear spin I_g = 5/2 becomes pronounced, giving rise to six asymmetric resonance lines in the absorption spectrum. Based on the nuclear transition, the sign of the principal axis of the EFG tensor is determined by the spectral analyses of ^{99}Ru Mössbauer spectra. In general, the EFG originates from contribution of unpaired electrons and local coordination environment. Since Ru^{4+} state is ignorable to contribution of unpaired electrons to the EFG tensors,[34,36] we discuss only the contribution of the local environment at the Ru site here. From the analysis of the spectrum, the sign of the EFG, V_{zz}, at ^{99}Ru nu-

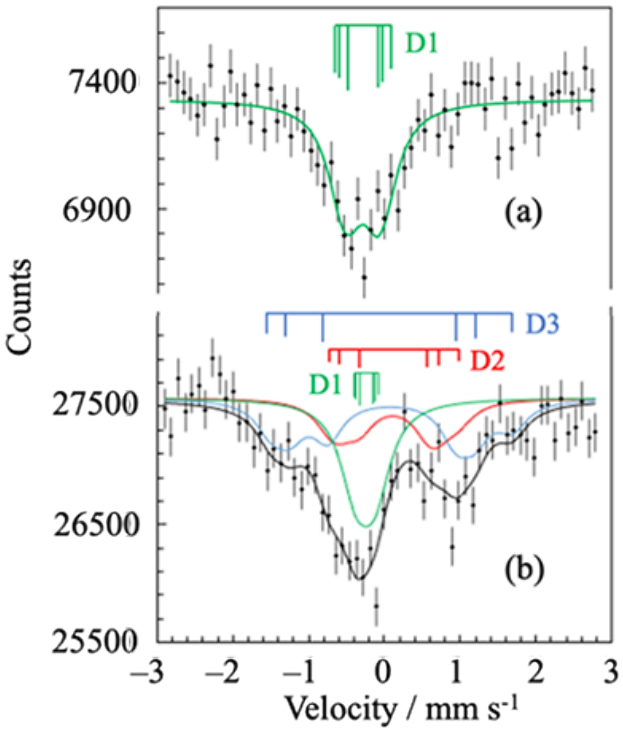

Figure 4. ^{99}Ru SR-based Mössbauer spectra of (a) Na_2RuO_3 and (b) Na-deficient $Na_{2-x}RuO_3$ obtained after charging measured at 7 K.

clei in Na_2RuO_3 was derived as negative. The principal axis of the EFG tensor was considered to be aligned with the *c*-axis. On the other hand, the crystallographic analysis of Na_2RuO_3 indicated that the RuO_6 octahedra had a large Jahn-Teller distortion.[32] The difference of the Ru-O bond length is about 7 % between the longest and shortest ones, suggesting that the RuO_6 octahedron is distorted along *c*-direction. The sign of the principal axis of the EFG tensor at ^{99}Ru nuclei agrees with that expected by the distortion of the RuO_6 octahedra.

Next, the ^{99}Ru Mössbauer spectrum of Na-deficient $Na_{2-x}RuO_3$ obtained after charging measured at 7 K is shown in Fig. 4 (b). The spectrum of $Na_{2-x}RuO_3$ showed significantly broader components than that of Na_2RuO_3, and new components were additionally observed. The differences of the spectra between them clearly demonstrate change of the oxidation states of Ru ions and coordination environment at the Ru sites due to electrochemical desodiation by charging. The spectrum was provisionally analyzed using three components of D1, D2 and D3. The obtained Mössbauer parameters of Na_2RuO_3 and Na-deficient $Na_{2-x}RuO_3$ after charging are summarized in Table 1.

D1 component, exhibiting a negative isomer shift with a small quadrupole splitting, was assigned to Ru^{4+} ions of the RuO_6 octahedra forming the honeycomb layer. Both D2 and D3 components showed positive isomer shifts and large quadrupole splittings. The value of the isomer shifts increases with the higher oxidation states of the Ru ions in ^{99}Ru Mössbauer spectroscopy, because the sign of ΔR/R is positive. It was considered that D2 and D3 components were attributed to Ru ions in higher oxidation states than the Ru4+ state. Since these isomer shifts lie between those of Ru^{4+} and Ru^{6+} observed in $BaRuO_4$,[31] the oxidation state of the species was quantitatively determined to be pentavalent. However, the stable compounds consisting of Ru^{5+} have only been reported for a limited number of systems, such as Na_3RuO_4, $Na_4Ru_2O_7$, and $M^{II}_2Ln^{III}RuO_6$ (M = alkaline earth metal, Ln = lanthanoid elements), and little information is available regarding the isomer shifts of Ru^{5+} species.[35,37] Recently, DeMarco *et al*. observed the temperature-dependent ^{99}Ru Mössbauer spectra of the ordered double perovskite Sr_2YRuO_6 and reported the isomer shift value of approximately +0.1 mm s^{-1} for Ru^{5+} state.[34] Therefore, taking into account the XRD results, D2 and D3 components could reasonably be assigned to a chemical species containing Ru^{5+} ions, namely the Na-deficient Na_1RuO_3 formed through electrochemical desodiation after charging. It is concluded that the oxidation state of some of Ru ions of Na_2RuO_3 was increased from Ru^{4+} to Ru^{5+} by charging.

Upon charging, the removal of Na ions from NaO_6 layers generated Na-vacancies and a contraction of the interlayer spacing parallel to *c*-axis, which induced the distortion of the RuO_6 octahedron that forms the honeycomb frame of $[Ru_{2/3}Na_{1/3}]O_2$ layers. It has been pointed out that there was significant variation in both the Ru-O and the O-O bond lengths in Na-deficient Na_1RuO_3.[14] Such structural distortions were considered to be the origin of the decrease in the quadrupole splitting of D1 component and the large ones observed in D2 and D3 components. The quadrupole splitting reflects both the d-electron configuration and the distortion of the crystal lattice. Assuming that both Ru^{4+} ($4d^4$) and Ru^{5+} ($4d^3$) form octahedral RuO_6 units, the octahedron of Ru^{4+}, which contains one unpaired electron, would be expected to exhibit a larger quadrupole splitting than that of Ru^{5+}, which has no unpaired electrons. However, our Mössbauer spectra obtained after charging produced the opposite result, suggesting that the contribution from lattice distortion is dominant. In order to provide a detailed interpretation of D1, D2 and D3 components, density functional theory (DFT) calculations are currently being conducted.

4. Conclusion

The improved ^{99}Ru SR-based Mössbauer spectroscopy enabled the elucidation of the local valence state and coordination environment at the Ru sites in Na_2RuO_3, a candidate cathode material for sodium-ion rechargeable batteries. Installation of appropriate channel-cut crystals improves the signal-to-noise ratio of the spectra. Improved thermal contact provided by boron nitride allowed the scatterer to be cooled to much lower temperatures, increasing the recoil-free fraction of the ^{99}Ru nuclei. Consequently, we succeeded in measuring ^{99}Ru Mössbauer spectra in shorter times and with higher statistical quality than conventional Mössbauer spectroscopy using a radioactive ^{99}Rh source.

Applying this improved technique to Na_2RuO_3 clearly revealed distinct changes in the Ru sites after electrochemical des-

TABLE 1. Summary of ^{99}Ru Mössbauer parameters of Na_2RuO_3 and Na-deficient $Na_{2-x}RuO_3$ obtained at 7 K after charging.

sample		δ^a / mm s^{-1}	$\Delta E_Q{}^b$ / mm s^{-1}	Area intensity / %
Na_2RuO_3		–0.29±0.06	–0.43±0.05	100
Na-deficient $Na_{2-x}RuO_3$	D1	–0.25±0.04	–0.13±0.14	34.1
	D2	0.07±0.06	–1.31±0.16	25.7
	D3	0.06±0.05	–2.45±0.13	40.2

[a] Isomer shift relative to Ru metal. [b] Quadrupole splitting defined by $e^2qQ_e/2$.
Linewidth Γ was fixed to be 0.48 mm s^{-1}.

odiation by charging. In Na-deficient $Na_{2-x}RuO_3$ formed after charging, Ru ions were identified for the first time as pentavalent states, resulting from one-electron oxidation. The isomer shift of Ru^{5+} was determined to be about 0.07 mm s^{-1}. In addition, X-ray diffraction and Mössbauer data indicated that the RuO_6 octahedra in Na-deficient $Na_{2-x}RuO_3$ were significantly distorted, leading to a large electric field gradient at the Ru nuclei.

The success of this work allows us to apply ^{99}Ru SR-based Mössbauer spectroscopy to probing redox-induced electronic and structural changes in Ru compounds. It also demonstrates that ^{99}Ru SR-based Mössbauer spectroscopy can be used to elucidate the physicochemical properties of Ru in a wide range of functional materials — for example, catalysts, magnetic and optical recording media, electronic components, and battery materials.

Acknowledgements

^{99}Ru SR-based Mössbauer spectroscopy experiments were conducted under the approval of JASRI (Proposal Nos. 2023B1373, 2024A1406), and the SPring-8 Budding Researchers Support Program (Proposal No. 2025A1591). The authors would like to express their gratitude to Prof. Shinichi Komaba and Dr. Shinichi Kumakura of Tokyo University of Science for providing the hard carbon used as an anode material for sodium-ion batteries, and to Mr. Takao Ochiai of the Technical Division at the University of Electro-Communications for his assistance in constructing the electronic circuits for the electrochemical charging experiments.

References

[1] S. L. Ruby, *J. Phys. (Paris), Colloq*. **35**, C6-209 (1974).
[2] M. Seto, R. Masuda, S. Higashitaniguchi, S. Kitao, Y. Kobayashi, C. Inaba, T. Mitsui, Y. Yoda, *Phys. Rev. Lett*. **102**, 217602 (2009).
[3] S. Tsutsui, R. Masuda, Y. Kobayashi, Y. Yoda, K. Mizuuchi, Y. Shimizu, H. Hidaka, T. Yanagisawa, H. Amitsuka, F. Iga, M. Seto, *J. Phys. Soc. Jpn*. **85**, 083704 (2016).
[4] R. Masuda, Y. Kobayashi, S. Kitao, M. Kurokuzu, M. Saito, Y Yoda, T. Mitsui, K. Hosoi, H. Kobayashi, H. Kitagawa, M. Seto, *Sci. Rep*. **6**, 20861 (2016).
[5] S. Tsutsui, H. Hanate, Y. Yoda, K. Matsuhira, *J. Phys. Soc. Jpn*. **90**, 083701 (2021).
[6] R. Masuda, Y. Kobayashi, S. Kitao, M. Kurokuzu, M. Saito, Y. Yoda, T. Mitsui, F. Iga, and M. Seto, *Appl. Phys. Lett*. **104**, 082411 (2014).
[7] R. Masuda, K. Kusada, T. Yoshida, S. Michimura, Y. Kobayashi, S. Kitao, H. Tajima, T. Mitsui, H. Kobayashi, H. Kitagawa, M. Seto, *Hyp. Int.* **240**, 120 (2019).
[8] O. C. Kistner, S. Monaro, R. Segnan, *Phys. Lett*. **5**, 299 (1963).
[9] O. C. Kistner, *Phys. Rev.* **144**, 1022 (1966).
[10] Mössbauer Effect Data Center, https://medc.dicp.ac.cn/Resources/Ru.htm (accessed Nov. 2025).
[11] K. M. Mogare, K. Friese, W. Klein, M. Jansen, *Z. Anorg. Allg. Chem*. **630**, 547 (2004).
[12] M. Tamaru, X. Wang, M. Okubo, A. Yamada, *Electrochem. Commun*. **33**, 23 (2013).
[13] P. Rozier, M. Sathiya, A-R. Paulraj, D. Foix, T. Desaunay, P-L. Taberna, P. Simon, J-M. Tarascon, *Electrochem. Commun*. **53**, 29 (2015).
[14] B. M. de Boisse, G. Liu, J. Ma, S. Nishimura, S-C. Chung, H. Kiuchi, Y. Harada, J. Kikkawa, Y. Kobayashi, M. Okubo, A. Yamada, *Nat. Commun*. **7**, 11397 (2016).
[15] M. H. N. Assadi, M. Okubo, A. Yamada, Y. Tateyama, *J. Mater. Chem. A* **6**, 3747 (2018).
[16] B. M. de Boisse, M. Reynaud, J. Ma, J. Kikkawa, S. Nishimura, M. Casas-Cabanas, C. Delmas, M. Okubo, A. Yamada, *Nat. Commun.* **10**, 2185 (2019).
[17] K. Jiang, X. Zhang, H. Li, X. Zhang, P. He, S. Guo, H. Zhou, *ACS Appl. Mater. Interfaces* **11**, 14848 (2019).
[18] X. Cao, H. Li, Y. Qiao, X. Li, M. Jia, J. Cabana, H. Zhou, Adv. *Energy Mater*. **10**, 1903785 (2020).
[19] M. G. T. Nathan, H. Yu, G.-T. Kim, J. Kim, J.-K. Kim, *Adv. Sci*. **9**, 2105882 (2022).
[20] N. Voronina, M-Y. Shin, H-J. Kim, N. Yaqoob, O. Guillon, S-H. Song, H. Kim, H-D. Lim, H-G. Jung, Y. Kim, H-K. Lee, K-S. Lee, K. Yazawa, K. Gotoh, P. Kaghazchi, S-T. Myung, *Adv. Ener. Mater.* **12**, 2103939 (2022).
[21] H. Katano, *Rev. Polarography*. **58**, 13 (2012).
[22] D. Bessas, D. G. Merkel, A. I. Chumakov, R. Rüffer, R. P. Hermann, I. Sergueev, A. Mahmoud, B. Klobes, M. A. McGuire, M. T. Sougrati, and L. Stievano, *Phys. Rev. Lett.* **113**, 147601 (2014).
[23] S. Kishimoto, Y. Yoda, M. Seto, S. Kitao, Y. Kobayashi, R. Haruki, T. Harami, *Nucl. Instrum. Methods Phys. Res. A* **513**, 193 (2003).
[24] S. Kishimoto, *Nucl. Instrum. Methods Phys. Res. A* **309**, 603 (2000).
[25] SPring-8 Bunch Mode Schedule, http://www.spring8.or.jp/ja/users/operation_status/schedule/bunch_mode (accessed Nov. 2025).
[26] M. Seto, R. Masuda, S. Higashitaniguchi, S. Kitao, Y. Kobayashi, C. Inaba, T. Mitsui, Y. Yoda, *J. Phys.: Conf. Ser*. **217**, 012002 (2010).
[27] F. J. Lynch F J, R. E. Holland and M. Hamermesh, *Phys. Rev*. **120**, 513 (1960).
[28] D. W. Hamill and G. R. Hoy, *Phys. Rev. Lett*. **21**, 724 (1968).
[29] Z. Klencsár, E. Kuzmann, A. Vértes, *J. Radioanal. Nucl. Chem*. **210**, 105 (1996); http://www.mosswinn.com/english/index.html (accessed Nov. 2025).
[30] Y. Kobayashi, T. Okada, K. Asai, M. Katada, H. Sano, F. Ambe, *Inorg. Chem*. **31**, 4570 (1992).
[31] N. N. Greenwood, T. C. Gibb, *"Mössbauer Spectroscopy"*, Chapman and Hall Ltd., p. 14, 503 (1971).
[32] L. S. I. Veiga, A. R. Overy, R. S. Perry, K. Yamaura, T. Mizokawa, K. Kobayashi, J. P. Attfield, *Phys. Rev. Mater.* **4**, 094202 (2020).
[33] T. C. Gibb, R. Greatrex, N. N. Greenwood, P. Kaspi, *J. Chem. Soc. D,* 319 (1971).
[34] M. DeMarco, G. Cao, J. E. Crow, D. Coffey, S. Toorongian, M. Haka, J. Fridmann, *Phys. Rev. B.*, 62, 14297 (2000).
[35] P. Gütlich, R. Link, A. Trautwein, *"Mössbauer Spectroscopy and Transition Metal Chemistry"*, Inorganic Chemistry Concepts Vol.3, Springer-Verlag, p. 113 (1978).
[36] T. C. Gibb, R. Greatrex, N. N. Greenwood, and K. G. Snowdon, *J. Solid State Chem*. **14**, 143 (1975).
[37] N. N. Greenwood, A. Earnshaw, "*Chemistry of the Elements* (2nd edition)", Elsevier, p. 1082 (2005).